Earthquake Engineering, Tenth World Conference © 1992 Balkema, Rotterdam. ISBN 90 5410 060 5

Comparison of seismic motions in two- and three-dimensional sedimentary basins

Masanori Horike & Yoshihiro Takeuchi
Osaka Institute of Technology, Japan

ABSTRACT: Seismic motion in two- and three-dimensional(2- and 3-D) irregularly layered sedimentary basins are computed by the Aki-Larner method and are compared to examine the effects of the number of dimensions and interface shape of basins. Input motions are vertically incident, plane S waves and two sedimentary basin models are prepared: one with a cosine-shaped basin-bedrock interface and the other with a trapezoid-shaped interface. Seismic motion in the 3-D basins is larger in amplitude and longer in duration than that in the corresponding 2-D basin. In particular, these features are much clearer in the wavefield of the trapezoid basin than in that of the cosine basin. Furthermore, the waveforms in the 3-D trapezoid model shows a strong spatial variation due to the interference of surface waves generated efficiently at the periphery.

1 INTRODUCTION

The considerable earthquake damage to Mexico city by the 1985 Mexicican earthquake reconfirmed the strong effect of surface geology on seismic motion. Many investigators have tried to reproduce seismic motion recorded in sedimentary basins, but achieved only partial success(Kudo, 1978; Horike, 1988; Vidale and Helmberger, 1988; Yamamoto et al., 1988; Yamanaka et al., 1989; Sasatani, 1990; Sato and Hasegawa, 1990). In these studies, the computed seismic motion was smaller in amplitude and shorter in duration than the recorded seismic motion. One cause of this discrepancy between the recorded and computed seismic motion is that the 2-D modeling does not reflect the actual 3-D subsurface structures of sedimentary basins. Therefore, it is meaningful to examine the difference between seismic motion in 3-D and 2-D sedimentary basins.

Many numerical methods have been developed for computation of seismic motion in irregularly layered structures: the wavefunction expansion method (e.g., Trifunac, 1971), the finite difference method (e.g., Boore, 1972), the Aki-Larner method (Aki and Larner, 1970), the finite element method (e.g., Lysmer and Drake, 1971), the boundary integral method (e.g., Wong and Jennings, 1975), the discrete wavenumber boundary element method (e.g., Bouchon, 1985), and the gaussian beam method (Cerveny, 1983). In principle, the methods listed above can be be extended for the computation of seismic motion in 3-D irregularly layered structures. However, because these methods have inherent weaknesses and strengths, we must choose the method depending on the configuration of the problems.

Bard and Bouchon (1985) classified sedimentary basin into two groups (shallow and deep) according to the ratio of the width to the maximum depth and showed that different wave phenomena occur in the two types of basins. Following their classification, most actual sedimentary basins are shallow ones. For the computation of seismic motion in shallow basins the Aki-Larner method (the AL method) is superior. Therefore, we employ the AL method for the numerical simulations in this study.

In this article, we first describe the extension of the AL method to the computation of seismic motion in 3-D sedimentary basins. Then, we compare seismic motion in 3-D and 2-D basins to examine the effect of the number of dimensions on seismic motion. Moreover, we compare seismic motion in two 3-D basin models to examine the effect of the interface shape. Finally, we draw several conclusions.

2 COMPUTATION METHOD

We outline the computation method. A detaied description can be found in Horike et al.(1990). Our problem is to calculate seismic motion on a flat free surface produced by the incidences of plane S waves. The configuration of the problem is shown in Fig. 1. The subsurface structure consists of a half space and a single overlying layer.

In the 3-D elastic wavefield, the displacement is represented as

$$\mathbf{u}(x,y,z) = \nabla\phi + \nabla\times\nabla\times(0,0,\psi) + \nabla(0,0,\chi), \quad (1)$$

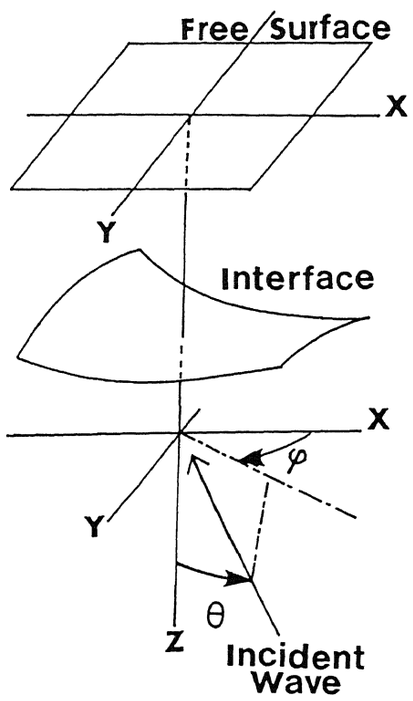

Fig. 1. Configuration of the problem. Parameters θ and φ denote the incident and azimuthal angles of the plane S wave. The medium consists of a sedimentary layer and a half space, separeted by an irregular surface.

where ϕ, ψ, and χ are P-, SV-, and SH-wave displacement potentials, respectively. Assuming spatial periodicity of the irregular interface with interval L_x and L_y in the two horizontal directions, the three potentals ϕ_1, ψ_1, and χ_1 in the layer are approximately expressed by the finite sum over two horizontal wavenumbers as

$$\phi_1 = \sum_{l=-N_x}^{N_x} \sum_{m=-N_y}^{N_y} \left(A_{lm}^{+} exp(i\nu_1 z) + A_{lm}^{-} exp(-i\nu_1 z)\right) exp\left(i(k_{xl}x + k_{ym}y)\right)$$

$$\psi_1 = \sum_{l=-N_x}^{N_x} \sum_{m=-N_y}^{N_y} \left(B_{lm}^{+} exp(i\gamma_1 z) + B_{lm}^{-} exp(-i\gamma_1 z)\right) exp\left(i(k_{xl}x + k_{ym}y)\right) \quad (2)$$

$$\chi_1 = \sum_{l=-N_x}^{N_x} \sum_{m=-N_y}^{N_y} \left(C_{lm}^{+} exp(i\gamma_1 z) + C_{lm}^{-} exp(-i\gamma_1 z)\right) exp\left(i(k_{xl}x + k_{ym}y)\right),$$

where $k_{xl} = 2\pi l/L_x + k_x^0$ and $k_{ym} = 2\pi m/L_y + k_y^0$, and $\nu_1 = (\omega^2/\alpha_1^2 - k_{xl}^2 - k_{ym}^2)^{1/2}$ and $\gamma_1 = (\omega^2/\alpha_1^2 - k_{xl}^2 - k_{ym}^2)^{1/2}$. Symbols α_1 and β_1 are P and S velocity in the layer. Integers i and m are respectively in the ranges of $-N_x \le l \le N_x$ and $-N_y \le m \le N_y$, where k_x^0 and k_y^0 are horizontal wavenumbers of incident plane wave.

In the half space, three displacement potentials ϕ_2, ψ_2, and χ_2 are respectively expressed as

$$\phi_2 = \sum_{l=-N_x}^{N_x} \sum_{m=-N_y}^{N_y} A_{lm}^{+} exp(i\nu_2 z) exp\left(i(k_{xl}x + k_{ym}y)\right) + \phi_0$$

$$\psi_2 = \sum_{l=-N_x}^{N_x} \sum_{m=-N_y}^{N_y} B_{lm}^{+} exp(i\gamma_2 z) exp\left(i(k_{xl}x + k_{ym}y)\right) + \psi_0 \quad (3)$$

$$\chi_2 = \sum_{l=-N_x}^{N_x} \sum_{m=-N_y}^{N_y} C_{lm}^{+} exp(i\gamma_2 z) exp\left(i(k_{xl}x + k_{ym}y)\right), + \chi_0$$

where $\nu_2 = (\omega^2/\alpha_2^2 - k_{xl}^2 - k_{ym}^2)^{1/2}$ and $\gamma_2 = (\omega^2/\beta_2^2 - k_{xl}^2 - k_{ym}^2)^{1/2}$. For the incident plane S waves, the potentials are

$$\phi_0 = 0$$

$$\psi_0 = E_0 exp\left(i(k_x^0 x + k_y^0 y - \gamma_z^0 z)\right) \quad (4)$$

$$\chi_0 = F_0 exp\left(i(k_x^0 x + k_y^0 y - \gamma_z^0 z)\right),$$

where $k_x^0 = \omega \sin\theta \cos\varphi/\beta_2$, $k_y^0 = \omega \sin\theta \sin\varphi/\beta_2$, and $\gamma_z^0 = \omega \cos\theta/\beta_2$. Employing the stress-free condition and the stress and displacement continuity on the interface, we obtain simultaneous linear equations for the coefficients A^+, B^+, C^+, D^+, E^+, and F^+. Solving these equations, and substituting thses coefficients into Eq. (2), we obtain the three displacement potentials. Moreover, substituting these potentials into Eq. (1) and setting z=0, we get the displacement on the free surface at frequencies (frequency responses). Seismic motion in the time domain is obtained by taking the reverse Fourier transform of the frequency responses.

3. COMPARISON

Two 3-D basin models are prepared. One has a cosine-shaped interface between the sediment and baserock (Fig. 2) and the other has a trapezoid-shaped interface (Fig. 3). The former has a smoothly curved interface, while the latter has a sharply curved one. The lengths of the long and short axes are the same for the two basins: 13 km and 6 km, respectively. The maximum depths are also the same: 0.5 km. The P- and S- wave velocities, densities, and quality factors are shown in Table 1.

For the comparison of seismic motion in 2-D and 3-D basins, we prepared 2-D basin models useing the cross-sections of the 3-D basin models just beneath

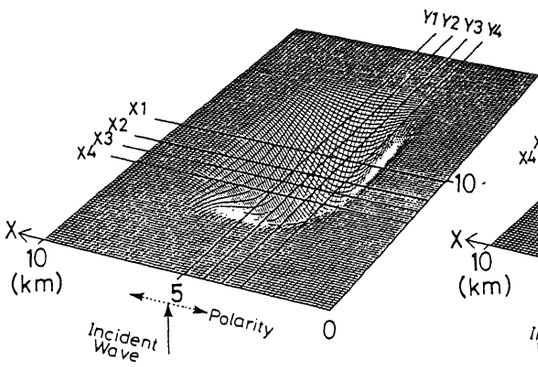

Fig. 2. 3-D cosine model. Lines X1 to X4 and Lines Y1 to Y4 denote the lines on which seismic motion are computed. The solid- and dashed-line arrows respectively denote the directions of the incidence and polarity.

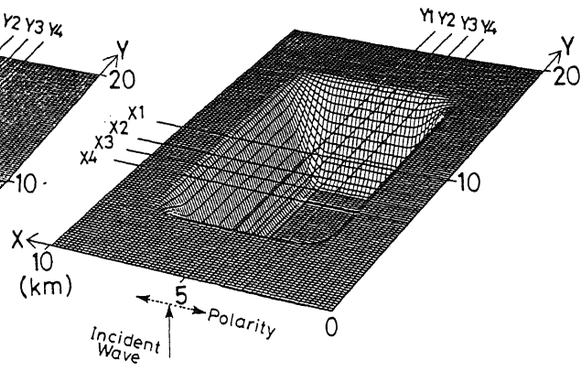

Fig. 3 3-D trapezoid model. The figure is the same as the figure 2 except for the shape of the basin-bedrock interface.

Table 1. List of medium parameters

Layer	P velocity (km/s)	S velocity (km/s)	Density (g/cm^3)	Q_p	Q_s
1	2.0	0.7	1.9	200	50
2	5.2	2.5	2.4	1000	300

the line Y1 (Fig. 2 and Fig. 3).

The input motions are vertically incident plane S waves polarized in the X direction. The waveform of the input motions in the time domain is a Ricker wavelet which is expressed as $\sqrt{\pi}/2(a-0.5)exp(-a)$, where $a = \left|\pi\left((t-t_0)/t_p\right)^2\right|$. The characteristic period t_p is 2.8s, which is equal to a fundamental predominant period.

3.1 *Effect of the number of basin dimensions*

3.1.1 *Cosine-shaped basin*

Figure 4 shows the X-component seismic motion on lines Y1, Y2, Y3, and Y4 which are denoted in Fig. 2. We readily find three clear phases in it. Phase A is an amplified S wave and phases B1 and B2 are the surface waves generated at the basin edges.

Figure 5 shows the X-component seismic motion in the 2-D cosine model. We compare this wavefield with the corresponding wavefield of the 3-D model (on Line Y1 in Fig.3) from the standpoint of wave-type, amplitude and duration.

The wave types contained in the 2-D wavefield are the same as those of the 3-D wavefield: amplified S wave (phase a), two surface waves (phases b1 and b2). We next compare the amplitude and duration of the main portion which consists of the three phases. The wavefield of the 3-D basin around the basin center (at sites Y= 10.5 km, 9.9 km, and 9.3 km on line Y1) is clearly larger in amplitude and longer in duration than that of the 2-D basin. This difference is mainly caused by marked excitation of secondary surface waves in the 3-D basin: surface waves in the 3-D basin are excited by the interface surface, whereas those in the 2-D basin are excited by the interface line. The above results show that the 3-D subsurface structure must be considered to obtain quantitative agreement between recorded and simulated seismic motion.

3.1.2 *Trapezoid-shaped basin*

Figure 6 shows the Y-component seismic motion on lines X1 to X4 in Fig. 3. We cannot find clear phases in this wavefield, because the waveforms strongly vary in space. For example, the seismic motion on lines X1 and X2, which are only 1.5 km apart, is quite different in amplitude, duration, and even frequency contents. This spatial variation is caused by the interference of the surface waves generated at the periphery of the basin and propagated in the X and Y directions.

We compare seismic motion on line Y1 with the corresponding seismic motion in the 2-D basin (Fig. 7). The waveforms of the 3-D wavefield are up to two times greater in amplitude and longer in duration than those of the 2-D wavefield. This difference is explained as follows: the interface of the 3-D basin excites the two surface waves propagating in the X and Y directions, whereas that of the 2-D basin excites the surface wave propagating only in the X direction. This result again shows that 3-D sub-surface structure must be considered to obtain a better agreement between the recorded and simulated seismic motion.

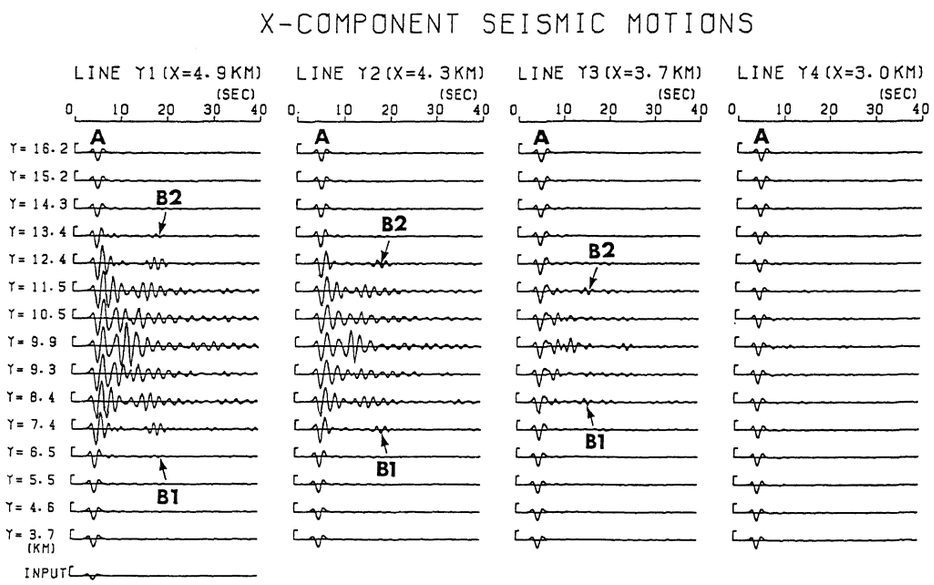

Fig. 4. X-component seismic motion on lines Y1 to Y4 in the cosine model. The lowermost trace is the incident Ricker wavelet.

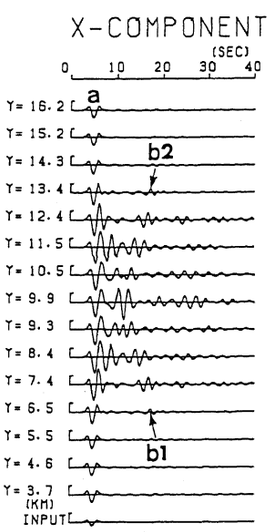

Fig. 5. Seismic motion in the 2-D cosine model. This wavefield corresponds to that on line Y1 in Fig. 4.

3.2 *Effect of the interface shape*

Finally, we examine the effect of interface shapes on seismic motion. Comparing the wavefield of the cosine-shaped basin (Fig. 4) with that of the trapezoid-shaped basin (Fig. 6), the latter is clearly much larger in amplitude and longer in duration. This shows that the interface shape greatly influences seismic motion. More specifically, a strongly curved portion of the intreface excites the secondary surface waves more efficiently than a gently curved one.

4 CONCLUSION

From the comparions of the wavefields in 3-D and 2-D sedimentary basins and of those in two different 3-D basins, we concluded that to obtain a better agreement between recorded and simulated seismic motion:

(1) three-dimensional subsurface structure must be considered.

(2) precise shape of the interface must be considered.

The second conclusion suggests the need of survey methods that unveil precise interface shapes.

REFERENCES

Aki, K. & K. Larner 1970. Surface motion of a lay-

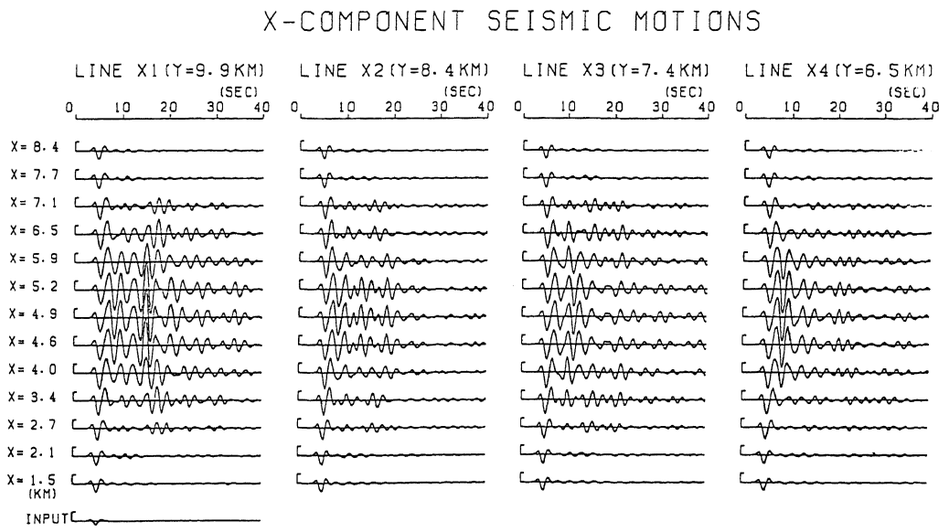

Fig. 6. X-component seismic motion on lines X1 to X4 in the 3-D trapezoid model.

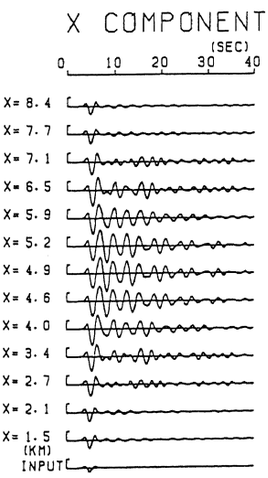

Fig. 7. Seismic motion in the 2-D trapezoid model. This wavefield corresponds to that on line X1 in Fig. 6.

ered medium having an irregular interface due to incident plane SH waves. *J. Geophys. Res.* 75: 934-954.

Bard, P.-Y. & M. Bouchon 1985. The two-dimensional response of sediment-filled valleys. *Bull Seism. Soc. Am.* 75: 519-541.

Boore, D. M. 1972. Finite difference methods for seismic propagation in heterogeneous materials. *Methods Comput. Phys.* 12: 1-31.

Bouchon, M. A simple complete numerical solution to the problems of diffraction of SH waves by an irregular surface. *J. Acoust. Soc. Am.* 77: 1-5.

Cerveny, V. 1983. Synthetic body wave seismograms for laterally varying layered structures by the Gaussian beam method. *J. R. Astron. Soc.* 73: 389-426.

Horike, M. 1988. Analysis and simulation of seismic ground motions observed by an array in a sedimantary basin. *J. Phys. Earth.* 36: 135-154.

Horike, M., H. Uebayashi. & Y. Takeuchi. 1990. Seismic response in three-dimensional sedimentary basin due to plane S wave incidence. *J. Phys. Earth.* 38: 261-284.

Kudo, K. 1978. The contribution of Love waves to strong ground motions. *Proc. 2nd international conference of microzonation*: 765-776.

Sasatani, T. 1990. Strong ground motions from intermediate-depth earthquake. *J. Fac. Sci. Hokkaido Univ. Ser. VII(geophysics).* 8: 449-464.

Sato, T. & M. Hasegawa. 1990. Formulation of hybrid approach for theoretical seismograms using thin layer element and axisymmetric finite element. *J. Struct. Constr. Eng.*. 414: 55-69.

Trifunac, M. D. 1971. Surface motion of a semicylindrical alluvial valley for incident plane SH waves. *Bull. Seism. Soc. Am.* 61: 1755-1770.

Vidale, J. E. & D. V. Helmberger. 1988. Elastic finite-difference modeling of the 1971 San Fernando, California earthquake. *Bull. Seism. Soc.*

Am. 78: 122-141.
Wong, H. L. & P. C. Jennings. 1975. Effect of Canyon topography on strong motion. *Bull. Seism. Soc. Am.* 65: 1239-1257.
Yamamoto, Y., Y. Hisada, & S. Tani. 1988. Long-period seismic motion in the Kanto plain. Part II: comparison of the recorded and computed waveforms. *Proc. Seism. Soc. Japan*: 172.
Yamanaka, H., K. Seo, & T. Samano. 1988. On the seismic motions observed in the south-west of the Kanto plain during an earthquake near the Izu-Oshima island, Japan. *Proc. national symposium on ESG*: 117-129.